A Combined Analysis of the Non-Gaussian Diffusion Methods in Monte Carlo Simulations, Anisotropic Fibre Phantoms, and in in vivo Human Brain Tissues

Farida A Grinberg[1], Ezequiel Farrher[1], Ivan I Maximov[1], and N. Jon Shah[1,2]
[1]*INM-4, Forschungszentrum Juelich, Juelich, Germany,* [2]*Department of Neurology, RWTH Aachen University, Aachen, Germany*

Target Audience. The target audience of this abstract are researchers investigating water diffusion properties in biological tissues.

Purpose

Diffusion magnetic resonance imaging permits non-invasive probing of tissue microstructure and function and provides invaluable information in brain diagnostics. Conventional methods are based on a simplified picture of Gaussian diffusion of water molecules in brain tissue characteristic of the isotropic non-confined liquids. However, complex cellular microstructure in the biological tissue, such as a brain, gives rise to non-Gaussian patterns of water diffusion. The propagation of water molecules tends to be affected by restrictions, compartmentalization, anisotropy, and is modulated by interfacial interactions with the cell membranes ("bound water") and exchange. Due to the heterogeneity and complexity of the tissue microstructure, the various contributions to the average MRI signal in *in vivo* studies cannot be easily resolved. Several phenomenological methods were suggested in the literature to describe the deviations from the Gaussian behaviour. However, such methods only seldom have been applied to the same experimental data [1]. The purpose of this work to perform a comparative analysis of the four non-Gaussian methods recently introduced in the brain research: a) the diffusion kurtosis imaging [2], DKI; b) the stretched-exponential function [3], SEF; c) the lognormal-distribution function [4], LNDF, and gamma-distribution function, GDF [5]. These functions were applied to the following systems: a) Monte Carlo diffusion simulations in a set of cylindrical objects, b) synthetic fibre phantoms with parallel and crossing fibres; c) in vivo human brain tissue. Monte Carlo simulations and physical phantoms allowed us to reduce the level of complexity of the real tissue and to analyse the influence of various factors, such as fibre packing density or a distribution of cylinder sizes, in a systematic way.

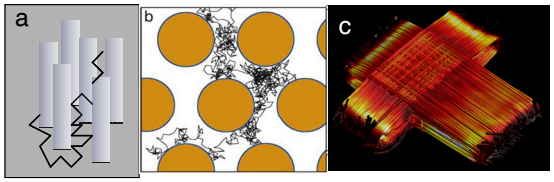

Figure 1. The model for MC simulations (a); interstitial space between the cylinders or fibres (b); fibre tracks in the fibre phantom with the gradient of fibre density and crossing fibres.

Materials and Methods

The construction of a fibre phantom with a fibre-density gradient and crossing-fibre regions is described in Ref. [6]. The diffusion attenuation curves used for the analysis were simulated for the model system (Figure 1) or measured experimentally using a double-refocused spin-echo pulse sequence in the fibre phantom and in *in vivo* human brains. The range of *b*-values was ≤ 7 μm^{-2} ms for LNDM, GDF and SEM, and $\leq$ 2.5 μm^{-2} ms for DKM.

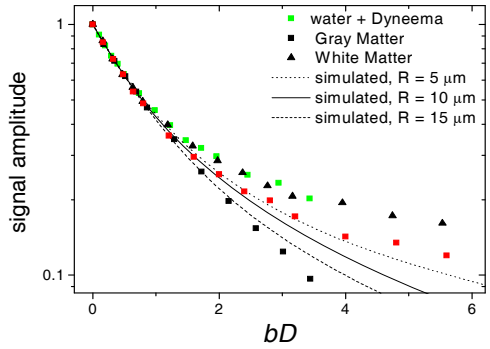

Figure2. Typical diffusion attenuation curves in various systems: GM, WM, fibre phantom, MC simulations. The initial slopes are normalized in order to emphasize the differences in the curves's shapes.

Results and Discussion

Figures 2 shows the typical non-exponential shapes of the diffusion attenuation curves of water in various systems: Monte Carlo simulations in the interstitial space between the cylinders (for various cylinder sizes), fibre phantom in the area of parallel fibres, in the gray and white matter voxels. All initial slopes (i.e. the apparent diffusivities) were normalised in order to better visualise the differences in the degree of non-monoexponentiality. An interesting observation is that these differences - in spite of differences in the microstructure of the investigated systems - become significant only after the signal attenuates by about 70% from its initial value. This suggests that more investigations are required with respect to the slow diffusion components in the brain tissue as they tend to be more sensitive to the tortuosity of the surrounding microstructure at typical diffusion times of the pulsed field gradient MRI experiments. The deviations from the Gaussian propagator were quantified with the help of above methods and the maps were produced for the fitting parameters. Figure 3 provides some examples of such maps for the phantom and for the *in vivo* human brain. In both systems, all methods were found complimentary to each other. In the phantom, different parameters exhibited different sensitivity to a fibre density and crossing fibres. In particular, a larger change in the "non-Gaussianity" parameter (MK) was accompanied with a smaller change in the mean diffusivity in DKI, whereas a larger change in the distributed diffusivity in SEM was related to a smaller change in stretching exponent α. In the brain tissue maps, different parameters exhibited different contrasts between WM and GM, and different sensitivity to partial volume effects. The results were supported by MC simulations.

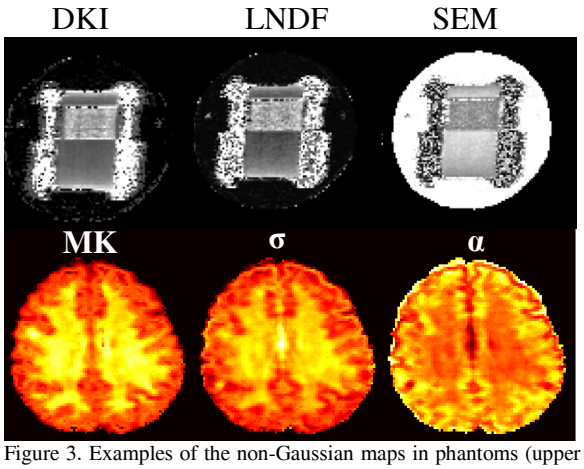

Figure 3. Examples of the non-Gaussian maps in phantoms (upper panel) and in *in vivo* brain tissue (bottom): MK (mean diffusion kurtosis in DKI); σ (the width of the distribution function in LNDM), α (the stretching exponent in SEM).

Conclusions

We demonstrated that all investigated methods provide complimentary information and different sensitivity with respect to the features such as fibre density in phantoms or partial volume effects in brain tissues. We discussed their relevance for better understanding potential diffusion contrasts in the fibrous tissue.

Acknowledgements

FG acknowledges valuable discussions with Dr. D.S. Grebenkov.

References

[1] Kristoffersen A. Statistical assessment of non-Gaussian diffusion models. Magn. Reson. Med., 2011; 66: 1639-48. [2] Jensen, J.H., Helpern, J.A., Ramani, A., et al., 2005. Diffusional kurtosis imaging: The quantification of non-gaussian water diffusion by means of magnetic resonance imaging. Magn. Reson. Med. 53, 1432-1440. [3] K.M. Bennett, K.M. Schmainda, R.T. Bennett, et al., Characterization of continuously distributed cortical water diffusion rates with a stretched-exponential model, Magn. Reson. Med., 50 (2003) 727-734. [4] F. Grinberg, L. Ciobanu, E. Farrher, N.J. Shah, Diffusion kurtosis imaging and log-normal distribution function imaging enhance the visualisation of lesions in animal stroke models, NMR Biomed., (2012). [5] Röding M, Bernin D, Jonasson J, et al. The gamma distribution model for pulsed-field gradient NMR studies of molecular-weight distributions of polymers. J Magn Reson, 2012; 222: 105-11. [6] E. Farrher, J. Kaffanke, A.A. Celik, T. Stocker, F. Grinberg, N.J. Shah, Novel multisection design of anisotropic diffusion phantoms, Magn. Reson. Imaging, 30 (2012) 518-526.